

UNCLASSIFIED

AD 436728

DEFENSE DOCUMENTATION CENTER

FOR

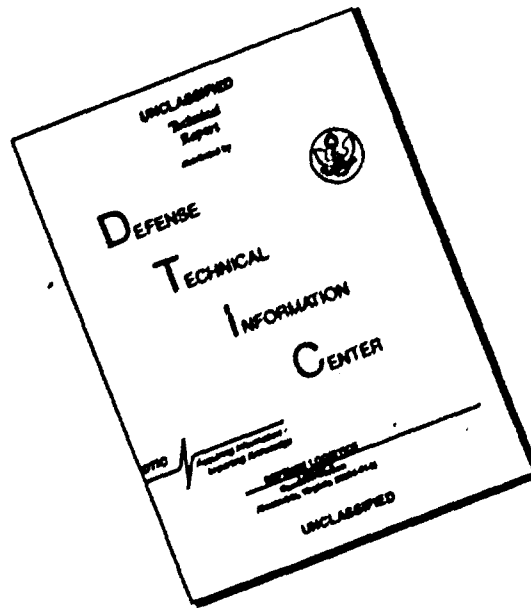
SCIENTIFIC AND TECHNICAL INFORMATION

CAMERON STATION, ALEXANDRIA, VIRGINIA



UNCLASSIFIED

# DISCLAIMER NOTICE



**THIS DOCUMENT IS BEST  
QUALITY AVAILABLE. THE COPY  
FURNISHED TO DTIC CONTAINED  
A SIGNIFICANT NUMBER OF  
PAGES WHICH DO NOT  
REPRODUCE LEGIBLY.**

NOTICE: When government or other drawings, specifications or other data are used for any purpose other than in connection with a definitely related government procurement operation, the U. S. Government thereby incurs no responsibility, nor any obligation whatsoever; and the fact that the Government may have formulated, furnished, or in any way supplied the said drawings, specifications, or other data is not to be regarded by implication or otherwise as in any manner licensing the holder or any other person or corporation, or conveying any rights or permission to manufacture, use or sell any patented invention that may in any way be related thereto.

436736

SSD-TDR-64-58

SEL-63-140

## Statistical Properties of Laser Sparkie Patterns

436736

by  
Joseph W. Goodman

December 1963

CATALOGED BY JDU  
AS AD NO.

### Technical Report No. 2303-1

Prepared under  
Air Force Contract AF04(695)-305, for  
Air Force Space Systems Division  
Air Force Systems Command  
United States Air Force

**SYSTEMS TECHNIQUES LABORATORY**  
**STANFORD ELECTRONICS LABORATORIES**

STANFORD UNIVERSITY • STANFORD, CALIFORNIA

NO. OTS



STATISTICAL PROPERTIES OF LASER SPARKLE PATTERNS

by

J. W. Goodman

December 1963

Reproduction in whole or in part  
is permitted for any purpose of  
the United States Government.

Technical Report No. 2303-1

Prepared under  
Air Force Contract AF04(695)-305  
for  
Air Force Space Systems Division  
Air Force Systems Command  
United States Air Force

Systems Techniques Laboratory  
Stanford Electronics Laboratories  
Stanford University      Stanford, California

FOREWORD

Technical Report No. 2303-1 was prepared by the Stanford Electronics Laboratories, Stanford University, on Air Force Contract AF04(695)-305 under Task No. 318201 of Project No. 3182, "University Program for Vehicle Detection and Defense." The work was administered under the direction of the Air Force Space Systems Division, Air Force Systems Command. Capt. Robert Eaglet was Project Engineer for the Division.

The studies presented covered the period from July through November 1963. The research activity was conducted by Joseph W. Goodman at the Systems Techniques Laboratory at Stanford.

This is an interim technical report on one phase of the work under Contract AF04(695)-305.

ABSTRACT

When laser light strikes a diffuse object, such as paper, the scattered light has been observed to possess a granular spatial structure. The statistical properties of these so-called "sparkle patterns," as seen by an observer in the far field of the scattering spot, are investigated.

The first order statistics of the observed electric-field strength, the observed light intensity, and the observed light phase are examined. The electric field is reasoned to be a complex normal random variable; the intensity a real, exponentially distributed random variable; and the phase a uniformly distributed random variable. Higher order statistics of these random processes are also discussed. The autocorrelation functions of the complex field and the intensity processes are investigated, and that of the electric field is found to be proportional to the Fourier transform of the light-intensity distribution incident on the scattering surface.

Spatial averages of the light intensity are considered and are found to converge to corresponding ensemble averages when either the area of the scattering spot or the averaging area grows large.

The influence of light spectral content on sparkle patterns is investigated in some detail. The cross correlation of patterns produced by different monochromatic light components is evaluated. The degree of correlation is found to depend on the frequency difference, the roughness of the scattering surface, the angle of incidence of the laser beam, and the position of the observer. Light spectral components of nonzero width are considered, and the influence of bandwidth on the ability of an observer to distinguish a sparkle pattern is examined. It is found that sparkle patterns exist for light of any bandwidth, but time-invariant patterns can be seen only when the bandwidth is less than a certain limit which depends on the roughness of the scattering surface, the angle of incidence of the laser beam, and the position of the observer.

---

Publication of this technical documentary report does not constitute Air Force approval of the report's findings or conclusions. It is published only for the exchange and stimulation of ideas.

CONTENTS

	<u>Page</u>
I. INTRODUCTION . . . . .	1
II. THE MODEL . . . . .	2
III. FIRST-ORDER STATISTICS OF THE SCATTERED LIGHT IN THE OBSERVATION PLANE . . . . .	6
A. An Expression for the Complex Field Strength in the Observation Plane . . . . .	6
B. Statistics of the Complex Field Strength . . . . .	7
C. Statistics of the Light Intensity and Phase . . . . .	8
IV. HIGHER ORDER STATISTICS OF THE SCATTERED LIGHT . . . . .	11
A. Intensity-Distribution Functions and Correlation Functions . . . . .	11
B. Higher Order Statistics of the Complex Field Strength . .	17
C. Second-Order Statistics of the Light Intensity and Phase . . . . .	19
V. SPATIAL AVERAGES . . . . .	24
VI. THE DEPENDENCE OF SPARKLE PATTERNS ON LIGHT FREQUENCY CONTENT . . . . .	28
A. The Cross Correlation of Patterns Produced by Different Frequency Components . . . . .	28
B. Statistical Properties of the Sparkle Pattern Produced by a Sum of Monochromatic Light Components . . . . .	32
C. Sparkle Patterns Produced by Spectral Components of Finite Width . . . . .	35
APPENDIX A. FAR-FIELD FOURIER TRANSFORM RELATIONS . . . . .	39
APPENDIX B. CROSS CORRELATION OF FIELD PATTERNS PRODUCED BY DIFFERENT FREQUENCY COMPONENTS . . . . .	42
APPENDIX C. FIRST-ORDER STATISTICS OF THE INTENSITY PATTERN PRODUCED BY A SUM OF WIDELY SPACED MONOCHROMATIC FREQUENCY COMPONENTS . . . . .	44
REFERENCES . . . . .	46



ILLUSTRATIONS

<u>Figure</u>	<u>Page</u>
1. The geometry of the scattering and observation planes . . .	4
2. Geometrical relationship between the laser beam, the scattering surface, and the observation plane . . . . .	30
3. Laser power spectrum with a single component . . . . .	36
4. Laser power spectrum with several components . . . . .	38
5. The geometry leading to Eq. (A.1) . . . . .	39

I. INTRODUCTION

A number of authors have recently commented on the granular "sparkle" patterns observed when a cw laser shines on a diffuse surface. Rigden and Gordon [Ref. 1] and Oliver [Ref. 2] have explained this granular pattern as a random scatter pattern which results from the "rough" character of the surface compared to the wavelengths involved. Langmuir [Ref. 3] has pointed out the striking similarity between this phenomenon and that of radar "clutter," a subject which has been extensively studied in the past [Ref. 4]. Although the nature of the clutter and sparkle phenomena are basically identical, some of the statistical properties that are important in the optical case have not been investigated previously. In this report, a relatively complete statistical theory of sparkle patterns is developed. In a companion report, the effects of sparkle on laser ranging and velocity-measurement systems will be investigated.

where  $D_0$  is the distance from the  $k^{\text{th}}$  scatterer to the observation point,

ervation

$|E_i|^2$  is the intensity of the light incident on the  $k^{\text{th}}$  scatterer, and

scatterer,

$|E_k|^2$  is the intensity of that portion of the light at the observation point which arises from the  $k^{\text{th}}$  scatterer.

e observa-

The scattering cross section is, in general, a function of both the light frequency and the observation point. It is assumed that the observation region is sufficiently small and the distance  $D_0$  sufficiently large so that  $s_k$  is constant within that region for any given frequency. By using the concept of cross section, the scattering elements are considered to be isotropic point radiators. Further assumptions on the statistical properties of the elementary scatterers will be discussed below.

h the  
the  
suffi-  
any given  
ing ele-  
assumptions  
l be dis-

At the scattering surface an "effective" scattered field distribution is defined by projecting the point radiators onto a plane X-Y at the surface, which is parallel to the observation plane U-V. A Z axis is defined running perpendicularly between the origin of the X-Y plane and the origin of the U-V plane, as shown in Fig. 1. The point  $z = 0$  is defined to coincide with the origin in the X-Y plane, while the origin of the U-V plane is assumed to lie at  $z = D$ , where  $D$  represents the distance between the two planes.

distribu-  
X-Y at  
A Z axis  
X-Y plane  
oint  $z = 0$   
le the  
D repre-

An effective complex field distribution for the projected scatterers in the X-Y plane may be written as

scatterers

$$E(x, y; t) = \sum_{k=1}^K \alpha_k \exp(j\beta_k) \delta(x - x_k, y - y_k) \exp(j\omega_0 t) \quad (2.2) \quad (2.2)$$

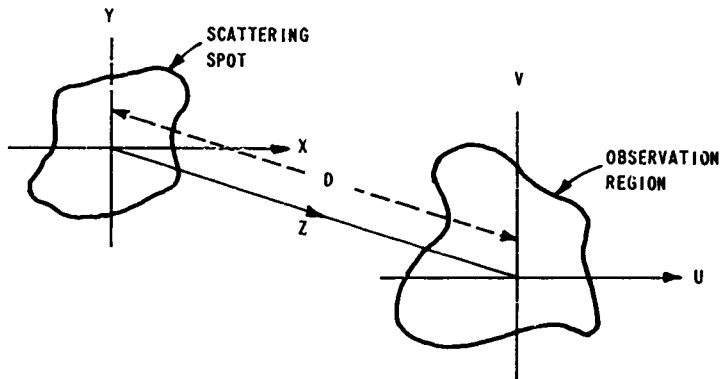


FIG. 1. THE GEOMETRY OF THE SCATTERING AND OBSERVATION PLANES.

where  $K$  is the number of scatterers contributing to the observed field in the  $U$ - $V$  plane;

$\alpha_k$  is equal to  $\sqrt{s_k/4\pi} |\underline{E}_i|$  and is a measure of the strength of the  $k^{\text{th}}$  scatterer;

$\beta_k$  is the phase of the radiation from the  $k^{\text{th}}$  scatterer, as measured at its projected point in the  $X$ - $Y$  plane;

$(x_k, y_k)$  is the location of the projection of the  $k^{\text{th}}$  scatterer in the  $X$ - $Y$  plane;

$\omega_0$  is the angular frequency of the electromagnetic radiation;  
and

$\delta(\cdot, \cdot)$  is a two-dimensional Dirac delta function.

To distinguish between the spatial and time variations of the field, Eq. (2.2) can be written

$$\underline{E}(x, y; t) = \underline{E}_0(x, y) \exp(j\omega_0 t) \quad (2.3)$$

from which it is evident that

$$\underline{E}_0(x, y) = \sum_{k=1}^K \sqrt{\frac{s_k}{4\pi}} |\underline{E}_1(x_k, y_k)| \exp(j\beta_k) \delta(x - x_k, y - y_k) \quad (2.4)$$

In the treatment which follows, the function  $\underline{E}_0(x, y)$  is considered to be a random process over an ensemble of possible scattering distributions in the X-Y plane. The following assumptions are made:

1. The scatterers are randomly distributed over the X-Y plane with uniform probability (as mentioned earlier).
2. The scattering cross section of a given scatterer is a random variable, and all scatterers have statistically independent and identically distributed cross sections.
3. Since nearly all surfaces are extremely "rough" compared to a light wavelength,\* the phase angles  $\beta_k$  are uniformly distributed in probability over the interval  $(0, 2\pi)$ .
4. Each  $\beta_k$  is statistically independent of all others.

The final assumption of statistical independence might be improved by allowing correlation to exist between the  $\beta$  of neighboring scatterers. However, providing that the correlation exists over an interval which is small compared to the total extent of the scattering "spot", no major changes in the results presented here are anticipated.

\*If the scattering surface is not rough compared to a wavelength, the results presented here apply only to that portion (possibly small) of the observed radiation which is not specular reflection. However, the results do apply to quasi-specular reflection from metallic objects caused by reflection from many small, optically smooth areas, each of which is randomly distributed in depth over several wavelengths.

### III. FIRST-ORDER STATISTICS OF THE SCATTERED LIGHT IN THE OBSERVATION PLANE

#### A. AN EXPRESSION FOR THE COMPLEX FIELD STRENGTH IN THE OBSERVATION PLANE

The relationship between the electric field in the X-Y plane at the scattering surface and the electric field in the observation region of the U-V plane is investigated in Appendix A. It is shown there that a Fourier transform relationship exists between the electric fields in the two planes; specifically, if  $\underline{\epsilon}(u, v; t)$  represents the complex electric field strength in the U-V plane, then

$$\underline{\epsilon}(u, v; t) = \frac{\exp \left[ j \left( \omega_0 t - \frac{2\pi D}{\lambda} \right) \right]}{j \lambda D} \exp \left[ -j \frac{\pi(u^2 + v^2)}{\lambda D} \right] \int_{-\infty}^{\infty} \int_{-\infty}^{\infty} \underline{E}_0(x, y) \exp \left[ j \frac{2\pi}{\lambda D} (ux + vy) \right] dx dy \quad (3.1)$$

provided the following conditions are met:

1.  $x/D \ll 1$  and  $y/D \ll 1$  for  $(x, y)$  in the scattering spot.
2.  $u/D \ll 1$  and  $v/D \ll 1$  for  $(u, v)$  in the observation region.
3.  $2\pi x^2/\lambda D \ll 1$  and  $2\pi y^2/\lambda D \ll 1$  (i.e., the observation region is in the far field of the scattering spot).
- 4.\*  $\pi u^4/4\lambda D^3 \ll 1$  and  $\pi v^4/4\lambda D^3 \ll 1$ .

For simplicity Eq. (3.1) is rewritten:

$$\underline{\epsilon}(u, v; t) = \underline{a} \exp(j\omega_0 t) \exp \left[ -j \frac{\pi(u^2 + v^2)}{\lambda D} \right] \underline{\epsilon}_0(u, v) \quad (3.2)$$

---

\*Note that this assumption does not require the scattering spot to be in the far field of the receiving optics (observation region).

where

$$\underline{\epsilon}_0(u, v) \triangleq \int_{-\infty}^{\infty} \int_{-\infty}^{\infty} \underline{E}_0(x, y) \exp \left[ j \frac{2\pi}{\lambda D} (ux + vy) \right] dx dy \quad (3.3)$$

and

$$\underline{a} \triangleq \frac{\exp \left( -j \frac{2\pi D}{\lambda} \right)}{j\lambda D} \quad (3.4)$$

The random parameters of the scattering surface become explicitly evident when (2.4) is substituted into (3.3), with the result

$$\underline{\epsilon}_0(u, v) = \sum_{k=1}^K \sqrt{\frac{s_k}{4\pi}} |E_1(x_k, y_k)| \exp \left\{ j \left[ \beta_k + \frac{2\pi}{\lambda D} (ux_k + vy_k) \right] \right\} \quad (3.5)$$

From this expression and the assumptions on the statistical properties of the scattering surface, it is now possible to derive the relevant statistical properties of the scattered light.

#### B. STATISTICS OF THE COMPLEX FIELD STRENGTH

From the expression (3.5) it is evident that the complex electric field  $\underline{\epsilon}_0(u, v)$  is given by a sum of randomly phased, random-amplitude phasors. Because of the statistical independence and uniform distribution of the random phases  $\beta_k$ , the following assertion can be proved [Ref. 5, p. 362]:

As the number  $K$  of elementary scatterers in the scattering spot increases without bound, the random process  $\underline{\epsilon}_0(u, v)$  becomes a complex normal process. The real and imaginary parts of this process are identically distributed with zero means and identical variances which will be designated  $\sigma^2/2$ . At any single point  $(u, v)$ , the real and imaginary parts of the process are statistically independent.

It is assumed throughout that the number of scattering elements within the spot is indeed so large that  $\underline{\epsilon}_0(u, v)$  may be considered to have normal statistics. Thus, if  $\underline{\epsilon}_0(u, v)$  is written as the sum of real and imaginary parts,

$$\underline{\epsilon}_0(u, v) = \epsilon_1(u, v) + j \epsilon_2(u, v) \quad (3.6)$$

the joint probability density function of  $\epsilon_1$  and  $\epsilon_2$  may be written as

$$p_{\epsilon_1, \epsilon_2}(\epsilon_1, \epsilon_2) = \frac{1}{\pi \sigma^2} \exp \left( - \frac{\epsilon_1^2 + \epsilon_2^2}{\sigma^2} \right) \quad (3.7)$$

From the relationship (3.2) between  $\underline{\epsilon}(u, v; t)$  and  $\underline{\epsilon}_0(u, v)$ , it can be seen that for a fixed  $(u, v; t)$  the former is also a normal process. However, as will be seen in Chapter IV, at any fixed instant of time,  $\underline{\epsilon}(u, v; t)$  in general will have statistics which are non-stationary over the U-V plane, while  $\underline{\epsilon}_0(u, v)$  is a stationary process.

#### C. STATISTICS OF THE LIGHT INTENSITY AND PHASE

The light intensity in the observation plane is defined as the square of the modulus of the complex electric field strength,

$$I(u, v) \triangleq |\underline{\epsilon}(u, v; t)|^2 \quad (3.8)$$

From (3.2) it is clear that

$$I(u, v) = |\underline{a}|^2 |\underline{\epsilon}_0(u, v)|^2 = |\underline{a}|^2 \left[ \epsilon_1^2(u, v) + \epsilon_2^2(u, v) \right] \quad (3.9)$$

The intensity is an important physical quantity to consider, in that the majority of light detectors have a response that is linearly proportional to intensity.



Although most detectors are insensitive to the phase of the received radiation, applications do exist in which the phase plays an important role (e.g., heterodyne receivers). Accordingly, the phase of the received radiation is defined by

$$\psi(u, v) = \tan^{-1} \frac{\epsilon_2(u, v)}{\epsilon_1(u, v)} \quad (3.10)$$

and its statistical properties, as well as those of the intensity, will be investigated.

To find the first-order statistics of  $I$  and  $\psi$ , the transformation defined by (3.9) and (3.10) must be applied to the random variables  $\epsilon_1$  and  $\epsilon_2$ . The inverse of this transformation is easily seen to be

$$\begin{aligned} \epsilon_1 &= \frac{I^{1/2}}{|\underline{a}|} \cos \psi \\ \epsilon_2 &= \frac{I^{1/2}}{|\underline{a}|} \sin \psi \end{aligned} \quad (3.11)$$

from which the Jacobian is found to be

$$|J| = \begin{vmatrix} \frac{\partial \epsilon_1}{\partial I} & \frac{\partial \epsilon_2}{\partial I} \\ \frac{\partial \epsilon_1}{\partial \psi} & \frac{\partial \epsilon_2}{\partial \psi} \end{vmatrix} = \frac{1}{2|\underline{a}|} \quad (3.12)$$

The joint probability density function of  $I$  and  $\psi$  may now be found from the relation [Ref. 6, p. 38]

$$p_{I, \psi}(I, \psi) = |J| p_{\epsilon_1, \epsilon_2} \left( \frac{I^{1/2}}{|\underline{a}|} \cos \psi, \frac{I^{1/2}}{|\underline{a}|} \sin \psi \right) \quad (3.13)$$

The result is

$$p_{I,\psi}(I, \psi) = \frac{1}{2\pi|\underline{a}|^2\sigma^2} \exp\left(-\frac{I}{|\underline{a}|^2\sigma^2}\right) \quad (3.14)$$

Integrating over the appropriate variables reveals the marginal densities of the intensity and phase to be

$$p_I(I) = \begin{cases} \frac{1}{|\underline{a}|^2\sigma^2} \exp\left(-\frac{I}{|\underline{a}|^2\sigma^2}\right) & I \geq 0 \\ 0 & \text{otherwise} \end{cases} \quad (3.15)$$

and

$$p_\psi(\psi) = \begin{cases} \frac{1}{2\pi} & 0 \leq \psi \leq 2\pi \\ 0 & \text{otherwise} \end{cases} \quad (3.16)$$

These results may be summarized as follows:

The light intensity  $I(u, v)$  is a real, exponentially distributed random variable, while the light phase  $\psi(u, v)$  is a uniformly distributed random variable on the interval  $(0, 2\pi)$ .

Note that

$$p_{I,\psi}(I, \psi) = p_I(I) p_\psi(\psi) \quad (3.17)$$

from which it follows that:

the intensity and phase at the point  $(u, v)$  are statistically independent random variables.

The moments of the intensity can be shown, from (3.15), to be

$$\overline{I^\nu} = |\underline{a}|^{2\nu} \sigma^{2\nu} \Gamma(\nu + 1) \quad (3.18)$$

#### IV. HIGHER ORDER STATISTICS OF THE SCATTERED LIGHT

##### A. INTENSITY-DISTRIBUTION FUNCTIONS AND CORRELATION FUNCTIONS

In the previous chapter the first-order statistics of the complex field strength, the intensity, and the phase of the scattered light were found. A complete statistical description of these quantities at any single point in space is known therefore, but not the statistical relationships between their values at two, three, or N different points in space (i.e., the "higher order" statistics). It is a remarkable property of the normal random process that once the so-called "auto-correlation function" of the process is known, the statistics of all orders are completely determined. In order to more fully describe the statistics of sparkle patterns, the concept of autocorrelation function and the related concept of "intensity-distribution function" are introduced.

The two-dimensional intensity-distribution function,  $S(x, y)$ , of the scattered light intensity at the point  $(x, y)$  is defined as the ensemble average of the scattered light intensity at that point. It is assumed that the elementary scatterers are so densely packed that  $S(x, y)$  may be considered to be a continuous function, in which case it can be seen that

$$S(x, y) = \frac{\bar{s}}{4\pi} |E_1(x, y)|^2 \quad (4.1)$$

where  $\bar{s}$  is the ensemble average of the scattering cross section of the elementary radiators. Thus the functional form of  $S(x, y)$  is identical, up to a multiplicative constant, with the functional form of the intensity distribution across the scattering spot. The intensity-distribution function has the particular property that, when integrated over the entire X-Y plane, it yields the constant  $\sigma^2$  which is twice the variance of the normal distributions discussed earlier.

The two-dimensional autocorrelation function of an arbitrary complex-valued random process  $\underline{\xi}(u, v)$  is defined by

$$\overline{R_{\underline{\xi}}}(\delta u, \delta v) = \overline{\underline{\xi}(u, v) \underline{\xi}^*(u - \delta u, v - \delta v)} \quad (4.2)$$

where the superbar indicates an ensemble average. A process is said to be wide sense stationary if the correlation function depends only on  $(\delta u, \delta v)$ ; while if it depends on  $(u, v)$  as well as  $(\delta u, \delta v)$ , the process is nonstationary.

The following important properties of any autocorrelation function should be noted:

1.  $\overline{R_{\underline{\xi}}}(\delta u, \delta v)$  is in general complex.
2.  $|\overline{R_{\underline{\xi}}}(\delta u, \delta v)| \leq |\overline{R_{\underline{\xi}}}(0, 0)|$ .
3.  $\overline{R_{\underline{\xi}}}(0, 0)$  is real and equals twice the average intensity of the process  $\underline{\xi}(u, v)$ .

Using the definition (4.2), the autocorrelation functions of the random processes  $\underline{\epsilon}_0(u, v)$ ,  $\underline{\epsilon}(u, v; t)$ , and  $I(u, v)$  will now be investigated. From (3.5) and (4.2) the autocorrelation function of  $\underline{\epsilon}_0(u, v)$  is

$$\overline{R_{\underline{\epsilon}_0}}(\delta u, \delta v) = \sum_{k=1}^K \overline{\frac{s_k}{4\pi}} \overline{|E_i(x_k, y_k)|^2 \exp \left[ j \frac{2\pi}{D\lambda} (x_k \delta u + y_k \delta v) \right]} \quad (4.3)$$

Note that this autocorrelation function does not depend on  $(u, v)$ , so the random process  $\underline{\epsilon}_0(u, v)$  is wide-sense stationary. Further note that if the scatterers are sufficiently dense in the scattering spot, the sum may be approximated by an integral, with the result

$$\overline{R_{\underline{\epsilon}_0}}(\delta u, \delta v) = \int_{-\infty}^{\infty} \int_{-\infty}^{\infty} \overline{\frac{s}{4\pi}} \overline{|E_i(x, y)|^2} \exp \left[ j \frac{2\pi}{D\lambda} (x \delta u + y \delta v) \right] dx dy \quad (4.4)$$

Recalling the definition (4.1) of the intensity-distribution function, it follows that:

The intensity-distribution function and the autocorrelation function of the random process  $\underline{\epsilon}_0(u, v)$  are a Fourier transform pair; specifically

$$\underline{R}_{\epsilon_0}(\delta u, \delta v) = \iint_{-\infty}^{\infty} S(x, y) \exp \left[ j \frac{2\pi}{\lambda} (x\delta u + y\delta v) \right] dx dy \quad (4.5)$$

Since the intensity-distribution function is proportional to the intensity of the incident light at the scattering surface, the functional form of the autocorrelation function can be found directly once the intensity distribution across the scattering spot is known. Note that for a given intensity-distribution function, the width of the corresponding autocorrelation function depends on the wavelength  $\lambda$ . The longer the wavelength, the wider the peak of the correlation function.

The autocorrelation function of  $\underline{\epsilon}(u, v; t)$  is now examined briefly. Equations (3.2) and (4.2) yield

$$\underline{R}_{\epsilon}(\delta u, \delta v) = |\underline{a}|^4 \underline{R}_{\epsilon_0}(\delta u, \delta v) \exp \left[ -j \frac{\pi}{\lambda D} (2u\delta u + 2v\delta v - \delta u^2 - \delta v^2) \right] \quad (4.6)$$

Since this expression is a function of  $(u, v)$  as well as  $(\delta u, \delta v)$ , the process  $\underline{\epsilon}(u, v; t)$  is nonstationary. However, it can be shown that if the scattering spot is in the far field of the observation region, then the dependence on  $(u, v)$  is eliminated and the process is wide-sense stationary.

Turning now to the autocorrelation function of the intensity random process, from (3.9) and (4.2) it is seen that

$$R_I(\delta u, \delta v) = |\underline{a}|^4 \overline{|\underline{\epsilon}_0(u, v)|^2 |\underline{\epsilon}_0(u - \delta u, v - \delta v)|^2} \quad (4.7)$$

Expanding  $\underline{\epsilon}_0(u, v)$  in its real and imaginary parts

$$\underline{\epsilon}_0(u, v) = \epsilon_1(u, v) + j \epsilon_2(u, v) \quad (4.8)$$

yields

$$\begin{aligned} R_I(\delta u, \delta v) = |\underline{a}|^4 & \left[ \overline{\epsilon_1^2(u, v) \epsilon_1^2(u - \delta u, v - \delta v)} \right. \\ & + \overline{\epsilon_2^2(u, v) \epsilon_2^2(u - \delta u, v - \delta v)} \\ & + \overline{\epsilon_2^2(u, v) \epsilon_1^2(u - \delta u, v - \delta v)} \\ & \left. + \overline{\epsilon_1^2(u, v) \epsilon_2^2(u - \delta u, v - \delta v)} \right] \quad (4.9) \end{aligned}$$

Now if  $x_1, x_2, x_3$ , and  $x_4$  are real, zero-mean, normal random variables, then the following relation is known to be true [Ref. 5, p. 343]:

$$\overline{x_1 x_2 x_3 x_4} = \overline{x_1 x_2} \overline{x_3 x_4} + \overline{x_1 x_3} \overline{x_2 x_4} + \overline{x_1 x_4} \overline{x_2 x_3} \quad (4.10)$$

Using this fact, it is not difficult to reduce (4.9) to

$$R_I(\delta u, \delta v) = |\underline{a}|^4 \left[ \sigma^4 + |\underline{\kappa}_{\underline{\epsilon}_0}(\delta u, \delta v)|^2 \right] \quad (4.11)$$

which provides a simple relation between the autocorrelation functions of  $\underline{\epsilon}_0(u, v)$  and  $I(u, v)$ . Note that the random process  $I(u, v)$  is wide-sense stationary.

Three important intensity-distribution functions and their corresponding autocorrelation functions are listed below:

### 1. Gaussian Scattering Spot

$$S(x, y) = \frac{\sigma^2}{2\pi \gamma_1 \gamma_2} \exp \left\{ -\frac{1}{2} \left[ \left( \frac{x}{\gamma_1} \right)^2 + \left( \frac{y}{\gamma_2} \right)^2 \right] \right\}$$

$$\underline{R}_{\varepsilon_0}(\delta u, \delta v) = \sigma^2 \exp \left\{ -\frac{1}{2} \left[ \left( \frac{\gamma_1 \delta u}{D\lambda} \right)^2 + \left( \frac{\gamma_2 \delta v}{D\lambda} \right)^2 \right] \right\} \quad (4.12)$$

$$R_I(\delta u, \delta v) = |\underline{a}|^4 \sigma^4 \left[ 1 + \exp \left\{ - \left[ \left( \frac{\gamma_1 \delta u}{D\lambda} \right)^2 + \left( \frac{\gamma_2 \delta v}{D\lambda} \right)^2 \right] \right\} \right]$$

### 2. Rectangular Scattering Spot

$$S(x, y) = \begin{cases} \frac{\sigma^2}{4XY} & \begin{cases} -X \leq x \leq X \\ -Y \leq y \leq Y \end{cases} \\ 0 & \text{otherwise} \end{cases}$$

$$\underline{R}_{\varepsilon_0}(\delta u, \delta v) = \sigma^2 \operatorname{sinc} \left( \frac{2X\delta u}{D\lambda} \right) \operatorname{sinc} \left( \frac{2Y\delta v}{D\lambda} \right) \quad (4.13)$$

$$R_I(\delta u, \delta v) = |\underline{a}|^4 \sigma^4 \left[ 1 + \operatorname{sinc}^2 \left( \frac{2X\delta u}{D\lambda} \right) \operatorname{sinc}^2 \left( \frac{2Y\delta v}{D\lambda} \right) \right]$$

where  $\operatorname{sinc} b \triangleq (\sin \pi b) / \pi b$ .

### 3. Circular Spot

$$S(x, y) = \begin{cases} \frac{\sigma^2}{\pi \rho^2} & 0 \leq x^2 + y^2 \leq \rho^2 \\ 0 & \text{otherwise} \end{cases}$$

$$\underline{R}_{\epsilon_0}(\delta u, \delta v) = 2\sigma^2 \frac{J_1\left(\frac{2\pi\rho}{\lambda D} \sqrt{(\delta u)^2 + (\delta v)^2}\right)}{\frac{2\pi\rho}{\lambda D} \sqrt{(\delta u)^2 + (\delta v)^2}} \quad (4.14)$$

$$\underline{\xi}_I(\delta u, \delta v) = |\underline{a}|^4 \sigma^4 \left\{ 1 + 4 \frac{J_1^2\left(\frac{2\pi\rho}{\lambda D} \sqrt{(\delta u)^2 + (\delta v)^2}\right)}{\left(\frac{2\pi\rho}{\lambda D}\right)^2 [(\delta u)^2 + (\delta v)^2]} \right\}$$

Finally, some quantities are defined which will be of considerable use in later chapters.

The cross-correlation function of two complex-valued random processes  $\underline{\xi}_1(u, v)$  and  $\underline{\xi}_2(u, v)$  is defined by

$$\underline{R}_{\underline{\xi}_{12}}(\delta u, \delta v) \triangleq \underline{\xi}_1(u, v) \underline{\xi}_2^*(u - \delta u, v - \delta v) \quad (4.15)$$

In words, the cross-correlation function provides a measure of the statistical similarity of the first random process  $\underline{\xi}_1$  at the point  $(u, v)$  and the second random process  $\underline{\xi}_2$  at the point  $(u - \delta u, v - \delta v)$ . A cross-correlation function need not have its maximum value at  $\delta u = \delta v = 0$ .

The cross-intensity-distribution function is defined as the two-dimensional Fourier transform of the cross-correlation function,

$$\underline{S}_{\underline{\xi}_{12}}(x, y) = \int_{-\infty}^{\infty} \int_{-\infty}^{\infty} \underline{R}_{\underline{\xi}_{12}}(\delta u, \delta v) \exp \left[ j \frac{2\pi}{\lambda D} (x\delta u + y\delta v) \right] d\left(\frac{\delta u}{\lambda D}\right) d\left(\frac{\delta v}{\lambda D}\right) \quad (4.16)$$



The cross-intensity-distribution function is in general a complex quantity.

## B. HIGHER ORDER STATISTICS OF THE COMPLEX FIELD STRENGTH

In this section the joint statistics of the real and imaginary parts of the complex field strength  $\epsilon_0$  at  $N$  different points in space are examined. Since these quantities have been seen to be normally distributed, the statistical properties of the field at  $N$  different points in space are completely described by a  $2N$ -dimensional normal distribution,

$$p_N(\epsilon_{11}, \epsilon_{12}, \epsilon_{21}, \epsilon_{22}, \dots, \epsilon_{N1}, \epsilon_{N2}) = \frac{\exp\left(-\frac{1}{2} \underline{\epsilon}_t \underline{\Lambda}^{-1} \underline{\epsilon}\right)}{(2\pi)^N |\underline{\Lambda}|^{1/2}} \quad (4.17)$$

where

$\epsilon_{k1}$  is the real part of the field strength at the  $k^{\text{th}}$  point;

$\epsilon_{k2}$  is the imaginary part of the field strength at the  $k^{\text{th}}$  point;

$\underline{\epsilon}$  is a column matrix of the  $\epsilon$ , defined by

$$\underline{\epsilon} = \begin{bmatrix} \epsilon_{11} \\ \epsilon_{12} \\ \epsilon_{21} \\ \epsilon_{22} \\ \vdots \\ \vdots \\ \vdots \\ \epsilon_{N1} \\ \epsilon_{N2} \end{bmatrix} \quad (4.18)$$

$\underline{\epsilon}_t$  is the transpose of  $\underline{\epsilon}$ ;

$\underline{\Lambda}$  is the covariance matrix of the  $\epsilon$ , defined by

$$\underline{\Lambda} = \overline{\underline{\epsilon} \underline{\epsilon}_t} = \begin{bmatrix} \overline{\epsilon_{11}\epsilon_{11}} & \overline{\epsilon_{11}\epsilon_{12}} & \cdots & \overline{\epsilon_{11}\epsilon_{N1}} & \overline{\epsilon_{11}\epsilon_{N2}} \\ \overline{\epsilon_{12}\epsilon_{11}} & \overline{\epsilon_{12}\epsilon_{12}} & \cdots & \overline{\epsilon_{12}\epsilon_{N1}} & \overline{\epsilon_{12}\epsilon_{N2}} \\ \vdots & \vdots & \ddots & \vdots & \vdots \\ \overline{\epsilon_{N1}\epsilon_{11}} & \overline{\epsilon_{N1}\epsilon_{12}} & \cdots & \overline{\epsilon_{N1}\epsilon_{N1}} & \overline{\epsilon_{N1}\epsilon_{N2}} \\ \overline{\epsilon_{N2}\epsilon_{11}} & \overline{\epsilon_{N2}\epsilon_{12}} & \cdots & \overline{\epsilon_{N2}\epsilon_{N1}} & \overline{\epsilon_{N2}\epsilon_{N2}} \end{bmatrix} \quad (4.19)$$

$\underline{\Lambda}^{-1}$  is the inverse of  $\underline{\Lambda}$ ; and

$|\underline{\Lambda}|$  is the determinant of  $\underline{\Lambda}$ .

The elements of the correlation matrix can be found from the autocorrelation function of the process  $\epsilon_0(u, v)$  by means of the following relationship, which is not difficult to prove;

$$\begin{aligned} \underline{R}_{\epsilon_0}(u_k - u_\ell, v_k - v_\ell) &= \overline{\epsilon_0(u_k, v_k) \epsilon_0^*(u_\ell, v_\ell)} \\ &= \left[ \overline{\epsilon_{k1}\epsilon_{\ell1}} + \overline{\epsilon_{k2}\epsilon_{\ell2}} \right] + j \left[ \overline{\epsilon_{\ell1}\epsilon_{k2}} - \overline{\epsilon_{\ell2}\epsilon_{k1}} \right] \quad (4.20) \\ &= 2 \overline{\epsilon_{k1}\epsilon_{\ell1}} + j 2 \overline{\epsilon_{\ell1}\epsilon_{k2}} = 2 \overline{\epsilon_{k2}\epsilon_{\ell2}} - j 2 \overline{\epsilon_{\ell2}\epsilon_{k1}} \end{aligned}$$

Note that the imaginary part of the autocorrelation function is proportional to the cross correlation between the real and imaginary parts of the field strength at the two different points involved. It was previously shown that the real and imaginary parts of the field strength at any one point are uncorrelated, but it is evident from (4.20) that the real and imaginary parts at different points may be correlated. If,

however, the laser spot is symmetrical about its center, the autocorrelation function is entirely real, and the real and imaginary parts of the field strength are statistically independent processes.

### C. SECOND-ORDER STATISTICS OF THE LIGHT INTENSITY AND PHASE

The second-order statistics of the intensity and phase may be found by a procedure similar to that used in Sec. IIIC. The transformation of interest is given by

$$\left. \begin{aligned} I_1 &= |a|^2 (\epsilon_{11}^2 + \epsilon_{12}^2) \\ I_2 &= |a|^2 (\epsilon_{21}^2 + \epsilon_{22}^2) \\ \psi_1 &= \tan^{-1} \frac{\epsilon_{12}}{\epsilon_{11}} \\ \psi_2 &= \tan^{-1} \frac{\epsilon_{22}}{\epsilon_{21}} \end{aligned} \right\} \quad (4.21)$$

where  $I_1$  and  $\psi_1$  are the intensity and phase at the point  $(u_1, v_1)$ , and  $I_2$  and  $\psi_2$  are the same quantities at  $(u_2, v_2)$ . The inverse of this transformation is

$$\left. \begin{aligned} \epsilon_{11} &= \frac{I_1^{1/2}}{|a|} \cos \psi_1 \\ \epsilon_{12} &= \frac{I_1^{1/2}}{|a|} \sin \psi_1 \\ \epsilon_{21} &= \frac{I_2^{1/2}}{|a|} \cos \psi_2 \\ \epsilon_{22} &= \frac{I_2^{1/2}}{|a|} \sin \psi_2 \end{aligned} \right\} \quad (4.22)$$

The Jacobian of the transformation can be shown to be

$$|J| = \frac{1}{4|\underline{a}|^4} \quad (4.23)$$

and, using the higher order analogy of (3.13),

$$p_{I_1 I_2 \psi_1 \psi_2}(I_1, I_2, \psi_1, \psi_2) = \frac{\exp\left(-\frac{1}{2}\underline{\varepsilon}_t \underline{\Delta}^{-1} \underline{\varepsilon}\right)}{16\pi^2 |\underline{a}|^4 |\underline{\Delta}|^{1/2}} \quad (4.24)$$

where in this case

$$\underline{\varepsilon} = \frac{1}{|\underline{a}|} \begin{bmatrix} I_1^{1/2} \cos \psi_1 \\ I_1^{1/2} \sin \psi_1 \\ I_2^{1/2} \cos \psi_2 \\ I_2^{1/2} \sin \psi_2 \end{bmatrix} \quad (4.25)$$

It is convenient at this point to have separate symbols for the real and imaginary parts of  $\underline{R}_{\underline{\varepsilon}_0}(\delta u, \delta v)$ . Accordingly,

$$\underline{R}_{\underline{\varepsilon}_0}(\delta u, \delta v) \triangleq R_1(\delta u, \delta v) + j R_2(\delta u, \delta v) \quad (4.26)$$

The covariance matrix can now be written

$$\underline{\Lambda} = \frac{1}{2} \begin{bmatrix} \sigma^2 & 0 & R_1 & R_2 \\ 0 & \sigma^2 & -R_2 & R_1 \\ R_1 & -R_2 & \sigma^2 & 0 \\ R_2 & R_1 & 0 & \sigma^2 \end{bmatrix} \quad (4.27)$$

The determinant  $|\underline{\Lambda}|$  is

$$|\underline{\Lambda}| = \frac{1}{16} \left( \sigma^4 - R_1^2 - R_2^2 \right)^2 \quad (4.28)$$

and the inverse matrix  $\underline{\Lambda}^{-1}$  can be shown to be

$$\underline{\Lambda}^{-1} = \frac{1}{2|\underline{\Lambda}|^{1/2}} \begin{bmatrix} \sigma^2 & 0 & -R_1 & -R_2 \\ 0 & \sigma^2 & R_2 & -R_1 \\ -R_1 & R_2 & \sigma^2 & 0 \\ -R_2 & -R_1 & 0 & \sigma^2 \end{bmatrix} \quad (4.29)$$

Carrying through the computation required by (4.24) yields

$$p_{I_1 I_2 \psi_1 \psi_2}(i_1, i_2, \psi_1, \psi_2) = \frac{\exp \left\{ -\frac{\sigma^2}{4|\underline{\Lambda}|^2 |\underline{\Lambda}|^{1/2}} (I_1 + I_2) + \frac{(I_1 I_2)^{1/2}}{2|\underline{\Lambda}|^2 |\underline{\Lambda}|^{1/2}} [R_1 \cos(\psi_2 - \psi_1) + R_2 \sin(\psi_2 - \psi_1)] \right\}}{16\pi^2 |\underline{\Lambda}|^4 |\underline{\Lambda}|^{1/2}} \quad (4.30)$$

Appropriate integrations over  $(\psi_1, \psi_2)$  and  $(I_1, I_2)$  yield the desired marginal densities [cf. Ref. 6, p. 163]

$$p_{I_1 I_2}(I_1, I_2) = \frac{\exp \left[ -\frac{\sigma^2}{4|\underline{a}|^2 |\underline{\Delta}|^{1/2}} (I_1 + I_2) \right]}{4|\underline{a}|^4 |\underline{\Delta}|^{1/2}} I_0 \left[ \frac{(I_1 I_2)^{1/2} (R_1^2 + R_2^2)^{1/2}}{2|\underline{a}|^2 |\underline{\Delta}|^{1/2}} \right] \quad (4.31)$$

and

$$p_{\psi_1 \psi_2}(\psi_1, \psi_2) = \frac{|\underline{\Delta}|^{1/2}}{4\pi^2 \sigma^4} \left[ \frac{(1 - \beta^2)^{1/2} + \beta(\pi - \cos^{-1} \beta)}{(1 - \beta^2)^{3/2}} \right] \quad (4.32)$$

where  $I_0$  is a modified Bessel function of the first kind, zero order; and where

$$\beta \triangleq \frac{R_1}{\sigma} \cos(\psi_2 - \psi_1) + \frac{R_2}{\sigma} \sin(\psi_2 - \psi_1) \quad (4.33)$$

and  $|\underline{\Delta}|$  is given by (4.28).

The random variable  $\Delta\psi$ , defined by

$$\Delta\psi = \psi_2 - \psi_1 \quad (4.34)$$

is a quantity of some interest. It represents the phase difference between the observed light at the points  $(u_2, v_2)$  and  $(u_1, v_1)$ . From (4.32) it is possible to show that

$$p_{\Delta\psi}(\Delta\psi) = \frac{|\underline{\Delta}|^{1/2}}{2\pi\sigma^4} \left[ \frac{(1 - \beta^2)^{1/2} + \beta(\pi - \cos^{-1} \beta)}{(1 - \beta^2)^{3/2}} \right] \quad (4.35)$$

where

$$\beta = \frac{R_1}{\sigma} \cos \Delta\psi + \frac{R_2}{\sigma} \sin \Delta\psi \quad (4.36)$$

Finally, the mean value of  $|\Delta\psi|$  is given by [Ref. 5, p. 411]

$$|\overline{\Delta\psi}| = \pi - 2 \sin^{-1} \left[ \frac{|R_{\varepsilon_0}(u_2 - u_1, v_2 - v_1)|}{\sigma^2} \right] \quad (4.37)$$

## V. SPATIAL AVERAGES

The preceding chapter considered only averages over an ensemble of scattering surfaces. However, the experimental tools that an observer must use are spatial averages (i.e., spatial integrations) over the observation region of the U-V plane. In this chapter the statistical properties of spatial averages are examined, with particular attention paid to discovering conditions under which spatial averages are, with high probability, very nearly the same as ensemble averages.

The integral of primary concern here is an average of the random process  $I(u, v)$  over the region

$$-U \leq u \leq U, \quad -V \leq v \leq V \quad (5.1)$$

of the observation plane. The average is defined by

$$\bar{I} \triangleq \frac{1}{4UV} \int_{-V}^V \int_{-U}^U I(u, v) du dv \quad (5.2)$$

First, the expected value (over the ensemble of scattering surfaces) of the spatial average is examined (5.2). The orders of expectation and integration may be interchanged to yield

$$\bar{\bar{I}} = \overline{I(u, v)} = |\underline{a}|^2 \sigma^2 \quad (5.3)$$

Thus the spatial integration yields, on the average, the ensemble expectation of  $I(u, v)$ .

It is pertinent at this point to inquire as to how large the departures of  $\bar{I}$  from its average value might be on any single trial. The dependence of these departures on  $U, V$  and on the statistical structure of  $I(u, v)$  is of particular interest. The answer to this question will, of course, indicate the magnitude of the difference between spatial averages of two intensity patterns which result from statistically independent scattering surfaces (composed of similar materials).



Therefore the variance of  $\bar{\lambda}$  over the ensemble of scattering surfaces is calculated.

To begin, note that

$$\overline{\lambda^2} = \frac{1}{16U^2V^2} \int_{-V}^V \int_{-U}^U \int_{-U}^U \int_{-V}^V \overline{I(u_1, v_1) I(u_2, v_2)} du_1 du_2 dv_1 dv_2 \quad (5.4)$$

which may be rewritten as

$$\overline{\lambda^2} = \frac{1}{16U^2V^2} \int_{-V}^V \int_{-U}^U \int_{-U}^U \int_{-V}^V R_I(u_1 - u_2, v_1 - v_2) du_1 du_2 dv_1 dv_2 \quad (5.5)$$

At this point it is clear that the variance of the spatial average will depend only on the averaging region and the autocorrelation function of  $I(u, v)$ .

Continuing, (4.11) may be used to write

$$\overline{\lambda^2} = |\underline{a}|^4 \sigma^4 + \frac{|\underline{a}|^4}{16U^2V^2} \int_{-V}^V \int_{-U}^U \int_{-U}^U \int_{-V}^V |\underline{R}_{\epsilon_0}(u_1 - u_2, v_1 - v_2)|^2 du_1 du_2 dv_1 dv_2 \quad (5.6)$$

from which it is seen that the variance of  $\bar{\lambda}$  is given by

$$\text{var } [\bar{\lambda}] = \frac{|\underline{a}|^4}{16U^2V^2} \int_{-V}^V \int_{-U}^U \int_{-U}^U \int_{-V}^V |\underline{R}_{\epsilon_0}(u_1 - u_2, v_1 - v_2)|^2 du_1 du_2 dv_1 dv_2 \quad (5.7)$$

A change of variables [Ref. 6, p. 68] allows the expression to be reduced to

$$\text{var } [\bar{\lambda}] = \frac{|\underline{a}|^4}{UV} \int_0^{2V} \int_0^{2U} \left(1 - \frac{\xi}{2U}\right) \left(1 - \frac{\eta}{2V}\right) |\underline{R}_{\epsilon_0}(\xi, \eta)|^2 d\xi d\eta \quad (5.8)$$

The expression (5.13) contains considerable information. One conclusion, which is not surprising, is the following:

As the size of the integration area ( $UV$ ) increases, the spatial average converges to the ensemble average of the intensity process.

A slightly more subtle, but related conclusion is:

As the size of the scattering spot (as measured by  $\gamma_1$  and  $\gamma_2$ ) increases, the spatial average again converges to the ensemble average.

## VI. THE DEPENDENCE OF SPARKLE PATTERNS ON LIGHT FREQUENCY CONTENT

In the previous chapters ideally monochromatic light sources were assumed. In actuality, the output of a laser, regardless of its type, consists typically of a number of spectral components, each of finite width. Since sparkle patterns were not observed until the advent of narrowband laser sources, it is of considerable interest to determine the exact role of spectral content in this phenomenon. This chapter is concerned with (1) the cross correlation between sparkle patterns produced by different monochromatic frequency components; (2) some statistical properties of sparkle patterns produced by a laser spectrum consisting of a number of monochromatic components; and (3) some sufficient conditions for observing sparkle patterns when the spectral components have nonzero width.

### A. THE CROSS CORRELATION OF PATTERNS PRODUCED BY DIFFERENT FREQUENCY COMPONENTS

Suppose that two light sources with different frequencies  $f_1$  and  $f_2$  cps are available. Each source is assumed to be ideally monochromatic, and will produce a sparkle pattern when its light falls on a diffuse surface. It is pertinent to inquire as to the correlation between the two patterns at each point  $(u, v)$  of the observation region, as a function of the frequency difference  $\Delta f$  defined by

$$\Delta f = f_2 - f_1 \quad (6.1)$$

assuming that in both cases the source illuminates the same area of a fixed target and that the intensity distributions of the incident spots are identical. If the correlation is high for all  $(u, v)$ , then the two sparkle patterns must be very nearly identical; if it is low, the two patterns bear little resemblance.

From the definition (4.15), the cross correlation of the intensity pattern when the frequency is  $f_1$  and the intensity pattern when the frequency is  $f_2$  is given by

$$\underline{R}_{I_{12}}(\delta u, \delta v) = \overline{I(u, v; f_1) I(u - \delta u, v - \delta v; f_2)} \quad (6.2)$$

By an argument similar to that used to derive (4.11) it can be shown that

$$\underline{R}_{I_{12}}(\delta u, \delta v) = |\underline{a}|^4 \left[ \sigma_1^2 \sigma_2^2 + |\underline{R}_{\epsilon_{12}}(\delta u, \delta v)|^2 \right] \quad (6.3)$$

where

$$\underline{R}_{\epsilon_{12}}(\delta u, \delta v) = \overline{\epsilon_0(u, v; f_1) \epsilon_0^*(u - \delta u, v - \delta v; f_2)} \quad (6.4)$$

while  $\sigma_1^2/2$  is the variance of the real and imaginary parts of  $\underline{\epsilon}_0(u, v; f_1)$ , and  $\sigma_2^2/2$  is the corresponding variance for  $\underline{\epsilon}_0(u, v; f_2)$ . If  $\Delta f$  is sufficiently small to assure that the same total intensity is scattered from the surface in both cases, then  $\sigma_1^2$  and  $\sigma_2^2$  are identical, and to determine  $\underline{R}_{I_{12}}$  it suffices to determine  $\underline{R}_{\epsilon_{12}}$ .

To continue, what is the correlation between the pattern  $I(u, v; f_1)$  and the untranslated pattern  $I(u, v; f_2)$  at each point  $(u, v)$ ? It is assumed, for simplicity, that the observation plane U-V is parallel to the plane defined by the mean surface (X-Y), although the laser beam is allowed to be incident on the surface at an angle  $\phi$  with the normal to the X-Y plane, as shown in Fig. 2. The Y and V axes are directed upward in this figure.

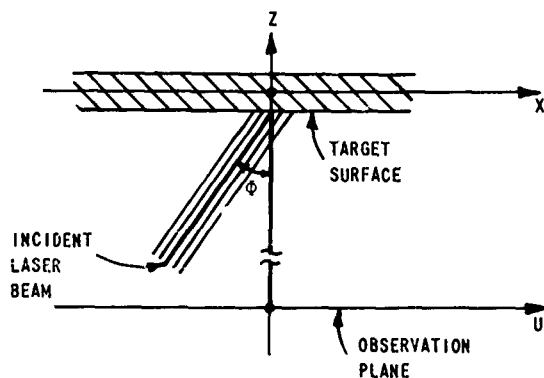


FIG. 2. GEOMETRICAL RELATIONSHIP BETWEEN THE LASER BEAM, THE SCATTERING SURFACE, AND THE OBSERVATION PLANE.

In Appendix B, the desired cross correlation is found to be given by the following expression:

$$\underline{R}_{\epsilon_{12}}(0, 0) = \underline{R}_{\epsilon_2}\left(\frac{\Delta f}{f_2} u, \frac{\Delta f}{f_2} v\right) \underline{\phi}_Z\left(\frac{\Delta f}{c \cos \phi} + \frac{\Delta f}{c}\right) \quad (6.5)$$

where

$$\underline{R}_{\epsilon_2}(\delta u, \delta v) \triangleq \underline{\epsilon}_0(u, v; f_2) \underline{\epsilon}_0^*(u - \delta u, v - \delta v; f_2) \quad (6.6)$$

and  $\underline{\phi}_Z(\xi)$  is the characteristic function of the random variables  $z_k$ , as given by the Fourier transform of the probability density function of the  $z_k$ ,

$$\underline{\phi}_Z(\xi) \triangleq \int_{-\infty}^{\infty} \exp(j2\pi\xi z_k) p_Z(z_k) dz_k \quad (6.7)$$

It is proposed to use the result (6.5) to find the conditions under which the two spatial patterns  $\epsilon_0(u, v; f_1)$  and  $\epsilon_0(u, v; f_2)$  will be highly correlated. For high correlation, both factors in (6.5) must be near their maximum values. The magnitude of the characteristic function,  $|\phi_Z(\xi)|$ , is considerably less than its maximum value when  $\xi$  is greater than the reciprocal of the standard deviation  $\sigma_Z$  of  $p_Z(z_k)$ . Thus a necessary condition for high correlation is\*

$$\Delta f < \frac{c}{\sigma_Z} \left( 1 + \frac{1}{\cos \phi} \right)^{-1} \quad (6.8)$$

Turning to the first factor in (6.5), it can be shown from (4.5) that  $|\bar{R}_{\epsilon_2}(\delta u, \delta v)|$  is considerably less than its maximum when

$$\delta u > \frac{Dc}{f_2 \ell_x} \quad \text{or} \quad \delta v > \frac{Dc}{f_2 \ell_y} \quad (6.9)$$

where  $\ell_x$  is the X-dimension width of the scattering spot and  $\ell_y$  is the Y-dimension width. Thus a necessary condition for high correlation is

$$u < \frac{Dc}{\Delta f \ell_x} \quad \text{and} \quad v < \frac{Dc}{\Delta f \ell_y} \quad (6.10)$$

for all  $(u, v)$  included in the observation region.

The conclusions of this section can be summarized as follows:

The correlation between patterns produced by different frequency components is maximum at  $(u, v) = (0, 0)$  and extends over a finite region of the U-V plane. The magnitude of the maximum correlation is determined by the relationship (6.8) between the frequency difference  $\Delta f$ , the surface roughness  $\sigma_Z$ , and the angle of incidence  $\phi$  of the laser beam.

---

\* This result is quite similar to the so-called Rayleigh Roughness Criterion [Ref. 4, p. 411].

## B. STATISTICAL PROPERTIES OF THE SPARKLE PATTERN PRODUCED BY A SUM OF MONOCHROMATIC LIGHT COMPONENTS

In this section the first-order statistics of the total intensity pattern are found for two special cases of interest, and an expression for the autocorrelation function of the total intensity pattern is also found.

It is assumed that the scattering process is a linear one, from which it follows that when the laser output consists of a sum of monochromatic frequency components, the total electric-field pattern is simply the sum of the field patterns produced by the individual components separately. The total electric field may be written, from (3.2), as

$$\underline{\epsilon}_T(u, v; t) = \underline{a} \sum_{n=1}^N \exp \left( j 2 \pi f_n t \right) \exp \left[ -j \frac{\pi f_n (u^2 + v^2)}{Dc} \right] \underline{\epsilon}_0(u, v; f_n) \quad (6.11)$$

where the  $f_n$  are the frequencies of the  $N$  monochromatic components involved.

The total intensity pattern is, from the definition (3.5), given by

$$I_T(u, v) = |\underline{a}|^2 \sum_{n=1}^N \sum_{m=1}^N \exp \left[ j 2 \pi (f_n - f_m) t \right] \exp \left[ -j \frac{\pi (f_n - f_m) (u^2 + v^2)}{Dc} \right] \underline{\epsilon}_0(u, v; f_n) \underline{\epsilon}_0^*(u, v; f_m) \quad (6.12)$$

If the intensity detector is followed by a low-pass filter sufficiently narrow to eliminate all but the dc term, (6.12) becomes

$$I_T^1(u, v) = \sum_{n=1}^N |\underline{a}|^2 |\underline{\epsilon}_0(u, v; f_n)|^2 = \sum_{n=1}^N I(u, v; f_n) \quad (6.13)$$

Now each  $I(u, v; f_n)$  is an exponentially distributed random variable which may or may not be significantly correlated with other members of the sum. For the general case of arbitrary frequency spacings between spectral components, the statistics of  $I_T^1(u, v)$  are extremely difficult to compute. However, two limiting cases of interest can be solved;

1. The case of spectral components with sufficiently wide frequency separations to produce uncorrelated\* patterns; and
2. The case of spectral components with sufficiently small frequency separations to produce perfectly correlated patterns.

Suppose first that the minimum separation between frequency components is so large that all terms of (6.13) are uncorrelated for every  $(u, v)$  in the observation region. A sufficient condition for this to be true is, from (6.8),

$$\min_{n \neq m} \{f_n - f_m\} \gg \frac{c}{\sigma_z} \left(1 + \frac{1}{\cos \phi}\right)^{-1} \quad (6.14)$$

Further suppose that the scattered light intensities resulting from different frequency components are not precisely identical, a condition which is always met in practice due to the fact that the laser spectral components will always have at least slightly different intensities. Then, as shown in Appendix C, the probability density function of the total intensity  $I_T^1(u, v)$  is given by a weighted sum of exponential functions,

$$p(I_T^1) = \begin{cases} \sum_{n=1}^N \frac{B_n}{|a|^2 \sigma_n^2} \exp\left(-\frac{I_T^1}{|a|^2 \sigma_n^2}\right) & I_T^1 \geq 0 \\ 0 & \text{otherwise} \end{cases} \quad (6.15)$$

where the  $B_n$  are real, constant weighting factors which are evaluated in Appendix C.

---

\*Because the random variables  $I(u, v; f_n)$  are composed of the sum of the squares of two normal processes, zero correlation implies statistical independence.



Next, suppose that the maximum separation between frequency components is so small that all terms of (6.13) have unity correlation in the observation region. Sufficient conditions for this to be true are

$$\max_{n,m} \{f_n - f_m\} \ll \frac{c}{\sigma_z} \left(1 + \frac{1}{\cos \phi}\right)^{-1} \quad (6.16a)$$

and

$$u \ll \frac{Dc}{\max_{n,m} \{f_n - f_m\} \lambda_x} \quad v \ll \frac{Dc}{\max_{n,m} \{f_n - f_m\} \lambda_y} \quad (6.16b)$$

for all  $(u, v)$  in the observation region. Since all the terms of (6.13) are perfectly correlated, the statistics of  $I_T^i(u, v)$  are easily seen to be exponential, with a probability density function given by

$$p(I_T^i) = \begin{cases} \frac{1}{|a|^2 \left(\sum_{n=1}^N \sigma_n\right)^2} \exp\left(-\frac{I_T^i}{|a|^2 \left(\sum_{n=1}^N \sigma_n\right)^2}\right) & I_T^i \geq 0 \\ 0 & \text{otherwise} \end{cases} \quad (6.17)$$

Finally the autocorrelation function of the total intensity pattern, as given by

$$R_T(\delta u, \delta v) = \overline{I_T^i(u, v) I_T^i(u - \delta u, v - \delta v)} = \sum_{n=1}^N \sum_{m=1}^N R_{I_{nm}}(\delta u, \delta v) \quad (6.18)$$

is investigated. From (6.3) it follows that

$$R_T(\delta u, \delta v) = \sum_{n=1}^N \sum_{m=1}^N |a|^4 \left[ \sigma_n^2 \sigma_m^2 + |R_{\epsilon_{nm}}(\delta u, \delta v)|^2 \right] \quad (6.19)$$

while from Appendix B it can be shown that if (6.16b) applies, then

$$\underline{R}_{\epsilon_{nm}}(\delta u, \delta v) \cong \underline{R}_{\epsilon_m}(\delta u, \delta v) \underline{\phi}_Z \left( \frac{f_n - f_m}{c \cos \phi} + \frac{f_n - f_m}{c} \right) \quad (6.20)$$

Thus,

$$R_T(\delta u, \delta v) = \sum_{n=1}^N \sum_{m=1}^N |\underline{a}|^4 \left[ \sigma_n^2 \sigma_m^2 + |\underline{p}_{nm}|^2 |\underline{R}_{\epsilon_{nm}}(\delta u, \delta v)|^2 \right] \quad (6.21)$$

where

$$\underline{p}_{nm} = \underline{\phi}_Z \left( \frac{f_n - f_m}{c \cos \phi} + \frac{f_n - f_m}{c} \right) \quad (6.22)$$

is independent of  $(\delta u, \delta v)$ . Thus:

the autocorrelation function of the total intensity pattern is given by a weighted sum of the autocorrelation functions of the individual intensity patterns.

#### C. SPARKLE PATTERNS PRODUCED BY SPECTRAL COMPONENTS OF FINITE WIDTH

Suppose that the laser output spectrum consists of a single spectral component of finite bandwidth  $W$ , as shown in Fig. 3. The exact shape of the spectrum is not of concern here, only the fact that it extends over a range  $W$  cps. In this section it is not required that a low-pass filter eliminate all the difference frequency terms, but rather the observation is performed directly on the output of the intensity detector.

The laser output field strength is considered to be a narrowband random process in time, which is represented as an amplitude-and phase-modulated sinusoid,

$$n(t) = A(t) \exp \{j[\omega_0 t + \theta(t)]\} \quad (6.23)$$

where  $n(t)$  = strength of the laser output

$A(t)$  = random amplitude modulation, of bandwidth  $W$  (approximately)

$\theta(t)$  = random phase modulation, of bandwidth  $W$  (approximately)

$\omega_0$  = center frequency of the laser spectrum.

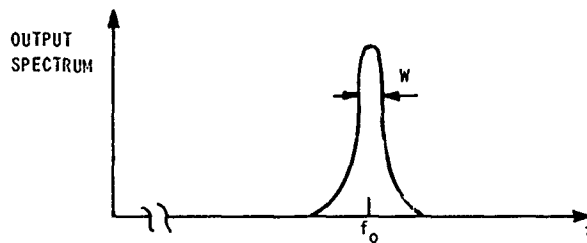


FIG. 3. LASER POWER SPECTRUM WITH A SINGLE COMPONENT.

The observer is assumed to examine the scattered intensity pattern for a time  $T$  sec. This observation interval is subdivided, for analysis purposes, into a number of subintervals, each of duration somewhat less than  $1/W$  sec. During any one of these subintervals the laser output is practically identical to a monochromatic sinusoidal oscillation of constant amplitude and constant frequency  $\omega$ , given by

$$\omega = \omega_0 + \dot{\theta} \quad (6.24)$$

where  $\dot{\theta}$  is the time derivative of the phase. Both the amplitude and the frequency of the oscillation will change as time progresses through the subintervals. Two distinctly different cases can now be distinguished:

Case 1

$$W \ll \frac{c}{\sigma_Z} \left( 1 + \frac{1}{\cos \phi} \right)^{-1} \quad (6.25a)$$

Case 2

$$W \gg \frac{c}{\sigma_Z} \left( 1 + \frac{1}{\cos \phi} \right)^{-1} \quad (6.25b)$$

In case 1, the maximum excursion of the oscillation frequency  $\omega$  is sufficiently small to assure that the intensity patterns produced in all subintervals are very highly correlated. Thus the sparkle-pattern structure does not change significantly from subinterval to subinterval, and an observer can distinguish a stationary sparkly pattern, regardless of how long his observation time  $T$  may be.

In case 2, the excursions of the oscillation frequency are so great that uncorrelated patterns may be produced in adjacent subintervals, and the sparkle pattern will "wash out" unless the observation time  $T$  is less than  $1/W$ . But note that no matter how wide  $W$  may be, for a sufficiently short observation time a distinct sparkle pattern will be observed.

In summary, sufficient conditions for observing sparkle patterns are

$$W \ll \frac{c}{\sigma_Z} \left( 1 + \frac{1}{\cos \phi} \right)^{-1} \quad (\text{regardless of } T) \quad (6.26a)$$

or

$$T \ll \frac{1}{W} \quad (\text{regardless of } \sigma_Z) \quad (6.26b)$$

The final situation to be examined is that of a laser spectrum consisting of a series of narrowband spectral components, as shown in Fig. 4. The total extent of the spectrum is denoted  $B$  cps, while the width of any one of the spectral components is approximately  $W$  cps.

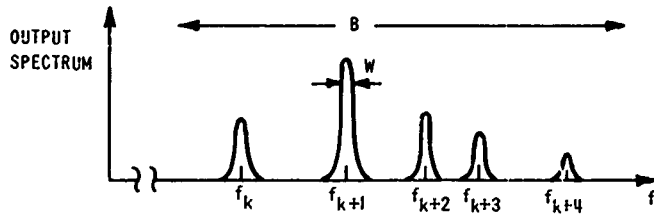


FIG. 4. LASER POWER SPECTRUM WITH SEVERAL COMPONENTS.

In this case the laser output may be written as a sum of narrowband processes,

$$n(t) = \sum_m A_m(t) \exp \{j[2\pi f_m t + \theta_m(t)]\} \quad (6.27)$$

where  $A_m(t)$  and  $\theta_m(t)$  are bandlimited to approximately  $W$  cps. Reasoning identical to that used for a single output component shows that the following conditions are sufficient for sparkle patterns to be distinguished:

$$1. \quad B \ll \frac{c}{\sigma_Z} \left(1 + \frac{1}{\cos \phi}\right)^{-1} \quad (6.28a)$$

or

$$2. \quad T \ll \frac{1}{W} \quad (6.28b)$$

In the present case it is not sufficient that

$$W \ll \frac{c}{\sigma_Z} \left(1 + \frac{1}{\cos \phi}\right)^{-1} \quad (6.29)$$

for under this condition it is still possible for different spectral components to produce uncorrelated patterns which will then add in proportions that change from subinterval to subinterval.

# APPENDIX A. FAR-FIELD FOURIER-TRANSFORM RELATIONS

This appendix considers the relationship between the field distribution  $\underline{E}(x, y; t)$  across the scattering spot and the field distribution  $\underline{e}(u, v; t)$  in the observation region. The observed field at the point  $(u, v)$  may be written as a sum of contributions from the incremental areas  $\Delta A = \Delta x \Delta y$  on the spot. As  $\Delta A$  is allowed to approach zero, the sum passes to an integral which may be written\*

$$\underline{e}(u, v; t) = \iint_{-\infty}^{\infty} \frac{\underline{E}(x, y; t)}{j\lambda r} \exp\left(-j \frac{2\pi r}{\lambda}\right) dx dy \quad (A.1)$$

where  $r$  is the distance from  $(x, y)$  to  $(u, v)$ . The geometry is shown in Fig. 5.

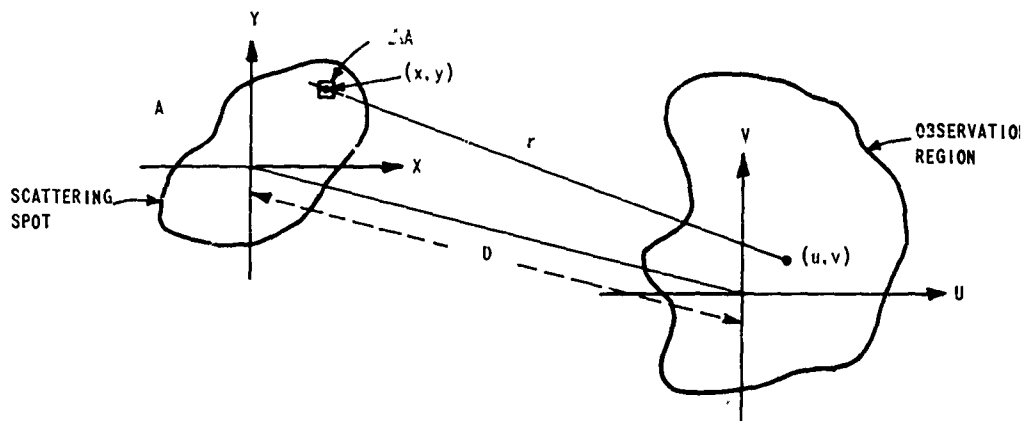


FIG. 5. THE GEOMETRY LEADING TO EQ. (A.1).

\*This equation follows directly from Huygen's principle.

Under the assumptions

$$\frac{x}{D} \ll 1, \quad \frac{y}{D} \ll 1 \quad \text{for all } (x, y) \text{ in scattering spot} \quad (\text{A.2a})$$

$$\frac{u}{D} \ll 1, \quad \frac{v}{D} \ll 1 \quad \text{for all } (u, v) \text{ in observation region} \quad (\text{A.2b})$$

(A.1) may be rewritten as

$$\underline{\varepsilon}(u, v; t) = \frac{\exp(j \omega_0 t)}{j \lambda D} \int_{-\infty}^{\infty} \int_{-\infty}^{\infty} \underline{E}_0(x, y) \exp\left(-j \frac{2\pi r}{\lambda}\right) dx dy \quad (\text{A.3})$$

where  $\underline{E}_0(x, y)$  is defined by

$$\underline{E}(x, y; t) = \underline{E}_0(x, y) \exp(j \omega_0 t) \quad (\text{A.4})$$

The distance  $r$  is seen to be given by

$$r = D \left\{ 1 + \left( \frac{u - x}{D} \right)^2 + \left( \frac{v - y}{D} \right)^2 \right\}^{1/2} \quad (\text{A.5})$$

The binomial expansion may now be used to expand the exponent in the integrand,

$$\begin{aligned} \frac{2\pi r}{\lambda} = \frac{2\pi D}{\lambda} & \left\{ 1 + \frac{1}{2} \left[ \left( \frac{u - x}{D} \right)^2 + \left( \frac{v - y}{D} \right)^2 \right] \right. \\ & \left. - \frac{1}{8} \left[ \left( \frac{u - x}{D} \right)^2 + \left( \frac{v - y}{D} \right)^2 \right]^2 + \text{higher order terms} \right\} \end{aligned} \quad (\text{A.6})$$

The observation region is defined to be in the far field of the scattering spot when

$$\text{and} \quad \left. \begin{aligned} 2\pi \frac{x^2}{D\lambda} &\ll 1 \\ 2\pi \frac{y^2}{D\lambda} &\ll 1 \end{aligned} \right\} \quad \begin{aligned} &\text{for all } (x, y) \\ &\text{in the scattering spot} \end{aligned} \quad (\text{A.7})$$

Assuming that these conditions hold, and further assuming that

$$\frac{\pi u^4}{4\lambda D^3} \ll 1$$

and

$$\frac{\pi v^4}{4\lambda D^3} \ll 1 \quad (\text{A.8})$$

Eq. (A.6) becomes

$$\begin{aligned} \underline{e}(u, v; t) &= \frac{\exp \left[ j \left( \omega t - \frac{2\pi D}{\lambda} \right) \right]}{j\lambda D} \exp \left[ -j \frac{\pi(u^2 + v^2)}{\lambda D} \right] \\ &\cdot \int_{-\infty}^{\infty} \int_{-\infty}^{\infty} \underline{e}_0(x, y) \exp \left[ j \frac{2\pi}{\lambda D} (ux + vy) \right] dx dy \end{aligned} \quad (\text{A.9})$$



APPENDIX B. CROSS CORRELATION OF FIELD PATTERNS  
PRODUCED BY DIFFERENT FREQUENCY COMPONENTS

This appendix investigates the cross-correlation function of two complex field patterns produced by different monochromatic frequency components. Following the notation of Chapter VI, the correlation function of interest is given by

$$\underline{r}_{\epsilon_{nm}}(\delta u, \delta v) = \underline{\epsilon}_0(u, v; f_n) \underline{\epsilon}_0^*(u - \delta u, v - \delta v; f_n) \quad (\text{B.1})$$

where

$$\begin{aligned} \underline{\epsilon}_0(u, v; f_j) = \sum_{k=1}^K \sqrt{\frac{s_k(f_j)}{4\pi}} |E_1(x_k, y_k)| \exp \left\{ j \left[ \beta_k(f_j) \right. \right. \\ \left. \left. + \frac{2\pi f_j}{Dc} (ux_k + vy_k) \right] \right\} \end{aligned} \quad (\text{B.2})$$

As the result of the statistical independence of the phases of different scatterers, Eqs. (B.1) and (B.2) can be combined to yield

$$\begin{aligned} \underline{r}_{\epsilon_{nm}}(\delta u, \delta v) = \sum_{k=1}^K \frac{\sqrt{s_k(f_n) s_k(f_m)}}{4\pi} \exp \{ j [\beta_k(f_n) - \beta_k(f_m)] \} \\ \cdot |E_1(x_k, y_k)|^2 \exp \left\{ j \left[ \frac{2\pi(f_n - f_m)}{Dc} (ux_k + vy_k) + \frac{2\pi f_m}{Dc} (x_k \delta u + y_k \delta v) \right] \right\} \end{aligned} \quad (\text{B.3})$$

which may be rewritten

$$\begin{aligned} R_{\epsilon_{nm}}(\delta u, \delta v) = \sum_{k=1}^K \frac{\sqrt{s_k(f_n) s_k(f_m)}}{4\pi} \exp \{j[\beta_k(f_n) - \beta_k(f_m)]\} \\ \cdot \overline{|E_1(x_k, y_k)|^2 \exp \left\{ j \left[ \frac{2\pi f_m}{Dc} \left\langle \left( \frac{f_n - f_m}{f_m} u + \delta u \right) x_k + \left( \frac{f_n - f_m}{f_m} v + \delta v \right) y_k \right\rangle \right] \right\}} \end{aligned} \quad (B.4)$$

But now note that

$$\exp \{j[\beta_k(f_n) - \beta_k(f_m)]\} = \exp \left[ j \frac{2\pi(f_n - f_m)}{c} \left( \frac{1}{\cos \phi} + 1 \right) z_k \right] = \phi_Z \left[ \frac{f_n - f_m}{c} \left( \frac{1}{\cos \phi} + 1 \right) \right] \quad (B.5)$$

where  $\phi$  is the angle of incidence of the laser beam (see Fig. 2),  $z_k$  is the Z coordinate of the  $k^{\text{th}}$  radiator, and  $\phi_Z(\xi)$  is the characteristic function of the random variables  $z_k$ . Finally, if the frequency difference  $f_n - f_m$  is sufficiently small to assure that the scattering cross sections of the elementary scatterers are independent of frequency, comparison of (B.4) and (4.3) shows that

$$R_{\epsilon_{nm}}(\delta u, \delta v) = R_{\epsilon_m} \left( \frac{f_n - f_m}{f_m} u + \delta u, \frac{f_n - f_m}{f_m} v + \delta v \right) \phi_Z \left[ \frac{f_n - f_m}{c} \left( \frac{1}{\cos \phi} + 1 \right) \right] \quad (B.6)$$

where

$$R_{\epsilon_m}(\delta u', \delta v') = \sum_{k=1}^K \frac{s_k}{4\pi} \overline{|E_1(x_k, y_k)|^2 \exp \left[ j \frac{2\pi f_m}{Dc} (x_k \delta u' + y_k \delta v') \right]} \quad (B.7)$$

is the autocorrelation function of the pattern corresponding to  $f_m$ .

APPENDIX C. FIRST-ORDER STATISTICS OF THE INTENSITY  
PATTERN PRODUCED BY A SUM OF WIDELY SPACED  
MONOCHROMATIC FREQUENCY COMPONENTS

In this appendix, the incident light beam is considered to be composed of a sum of monochromatic spectral components, spaced so widely apart that the intensity patterns produced by different components are statistically independent. As indicated by Eqs. (3.11) and (6.13), the total intensity pattern is simply the sum of a number of statistically independent, exponentially distributed random variables.

It is a well-known result of statistics that the characteristic function of a sum of a number of statistically independent random variables is simply the product of the characteristic functions of the component random variables. From (3.11), the  $n^{\text{th}}$  component intensity pattern has a probability density function given by

$$p(I_n) = \begin{cases} \frac{1}{|a|^2 \sigma_n^2} \exp\left(-\frac{I_n}{|a|^2 \sigma_n^2}\right) & I_n \geq 0 \\ 0 & \text{otherwise} \end{cases} \quad (\text{C.1})$$

The corresponding characteristic function is [Ref. 7, p. 221]

$$\underline{\phi}_n(\xi) = \frac{1}{(1 - j 2\pi |a|^2 \sigma_n^2 \xi)} \quad (\text{C.2})$$

It follows that the characteristic function of the total intensity pattern is

$$\underline{\phi}_T(\xi) = \prod_{n=1}^N \frac{1}{(1 - j 2\pi |a|^2 \sigma_n^2 \xi)} \quad (\text{C.3})$$

where  $N$  is the number of frequency components involved. Now if none of the  $\sigma_n$  are identical, the characteristic function has only single-order poles, and a partial-fraction expansion yields the simple result

$$\underline{\phi}_T(\xi) = \sum_{n=1}^N \frac{B_n}{1 - j \, 2\pi \, |\underline{a}|^2 \sigma_n^2 \xi} \quad (C.4)$$

where

$$B_n = \lim_{j\xi \rightarrow \left(2\pi |\underline{a}|^2 \sigma_n^2\right)^{-1}} \left(1 - j \, 2\pi \, |\underline{a}|^2 \sigma_n^2 \xi\right) \underline{\phi}_T(\xi) \quad (C.5)$$

An inverse Fourier transform of (C.4) yields the probability density function of the total intensity pattern,

$$p(I_T) = \begin{cases} \sum_{n=1}^N \frac{B_n}{|\underline{a}|^2 \sigma_n^2} \exp\left(-\frac{I}{|\underline{a}|^2 \sigma_n^2}\right) & I \geq 0 \\ 0 & \text{otherwise} \end{cases} \quad (C.6)$$

## REFERENCES

1. J. D. Rigden and E. I. Gordon, "The Granularity of Scattered Optical Maser Light," Proc. IRE, 50, 11, Nov 1962, p. 2367.
2. B. M. Oliver, "Sparkling Spots and Random Diffraction," Proc. IEEE, 51, 1, Jan 1963, p. 220.
3. R. V. Langmuir, "Scattering of Laser Light," Appl. Phys. Lett., 2, 2, 15 Jan 1963.
4. Propagation of Short Radio Waves, Rad. Lab. Series, Vol. 13, L. N. Ridenour, ed., McGraw-Hill Book Co., New York, 1951.
5. D. Middleton, Statistical Communication Theory, McGraw-Hill Book Co., New York, 1960.
6. W. B. Davenport and W. L. Root, Random Signals and Noise, McGraw-Hill Book Co., New York, 1958.
7. E. Parzen, Modern Probability Theory and Its Applications, John Wiley & Sons. New York, 1960.

SYSTEMS TECHNIQUES DISTRIBUTION LIST  
February 1964

<p>Commanding Officer USAEIRDL Fort Monmouth, N.J. 1 Attn: SELRA/LNR 1 Attn: SELRA/OR 1 Attn: SELRA/SER 1 Attn: SELRA/SN 1 Attn: SELRA/SA 1 Attn: SELRA/SHD 1 Attn: SELRA/SEA 1 Attn: SELRA/SEJ 1 Attn: SELRA/SES 1 Attn: SELRA/SEE 1 Attn: SELRA/SE 1 Attn: SELRA/ADT 1 Attn: SELRA/ADO</p> <p>Commanding Officer USAEIRDL, Evans AFB El Paso, N.J. 1 Attn: Chief, Adv. Tech. Br. SEA</p> <p>Commanding General, USASCS Fort Monmouth, N.J. 1 Attn: H. Allen, EW Div.</p> <p>Commanding General U.S. Army Missile Command Redstone Arsenal, Ala. 1 Attn: AMSMI-YRT</p> <p>Commanding Officer U.S. Army Signal Missile Support Agency White Sands Missile Range, N.M. 1 Attn: SIGSS-MEW 1 Attn: SIGSS-PC</p> <p>Commanding General U.S. Army Electronics Proving Ground Fort Huachuca, Ariz. 1 Attn: Tech. Library</p> <p>Army Electronics Lab Liaison Office-WIT 77 Mass. Ave., Rm 26-131 Cambridge 39, Mass. 1 Attn: RLE Document Room</p> <p>Army Research Liaison Office Lincoln Lab-WIT 1 Lexington 73, Mass.</p> <p>Commanding Officer Office of Naval Research Br. Off. 1000 Geary St. San Francisco, Calif. 1 Attn: Mr. J. Froman</p> <p>Director, U.S. Naval Res. Lab Washington 25, D.C. 1 Attn: Code 2027 1 Attn: Code 5430 1 Attn: Code 2000</p> <p>Chief of Naval Operations Electronic Warfare Systems Br. Washington 25, D.C. 1 Attn: Code Op-352 2 Attn: Code Op-07T4</p> <p>Commanding Officer and Director U.S. Naval Electronics Lab. San Diego 52, Calif. 1 Attn: Library 1 Attn: 3060 1 Attn: 3260 1 Attn: 3320</p> <p>Commander U.S. Naval Missile Ct. Pt. Mugu, Calif. 1 Attn: N03022</p>	<p>Commanding General U.S. Army Materiel Command Washington 25, D.C. 1 Attn: AMCRD-DE-E 1 Attn: AMCRD-RS-PE-E</p> <p>Bureau of Naval Weapons Dept. of the Navy Washington 25, D.C. 1 Attn: RAAV-11 1 Attn: RAAV-6</p> <p>Navy Department U.S. Naval Avionics Facility Indianapolis 18, Ind. 1 Attn: Station Library</p> <p>Director of Res. and Tech., USAF Washington 25, D.C. 1 Attn: AFIA7-ER</p> <p>Chief of Naval Research Dept. of the Navy Washington 25, D.C. 2 Attn: Code 463 1 Attn: Code 427</p> <p>Chief, Bureau of Ships Dept. of the Navy Washington 25, D.C. 1 Attn: Code 362C 1 Attn: Code 680</p> <p>Commander, ASD Wright-Patterson AFB, Ohio 1 Attn: ASNPRO 1 Attn: ASRNR-21, (Mr. Bayliss) 1 Attn: ASRNR-32 1 Attn: ASNORR 1 Attn: ASNPRS-5</p> <p>Air Force Avionics Laboratory Research and Technology Div. Also, USAF Wright-Patterson AFB, Ohio, 45433 2 Attn: AFWW, Capt. J. S. Butto</p> <p>FTD Wright-Patterson AFB, Ohio, 45433 1 Attn: TDEE 1 Attn: TDCE, Mr. T. M. Hay, Jr.</p> <p>Executive Director Air Force Office of Scientific Res. Washington 25, D.C. 1 Attn: SRFE</p> <p>APGC (PGAPI) 1 Eglin AFB, Fla.</p> <p>Commander Air Force Missile Dev. Center Holloman AFB, N.M. 1 Attn: MDR</p> <p>Commander, RADC Griffiss AFB Rome, N.Y. 1 Attn: RAWCL 1 Attn: RAALD, Doc. Lib. 1 Attn: RALS, J. Fallik 1 Attn: RALSS, M. Diab 1 Attn: RAWEC, T. J. Domurat 1 Attn: RAWED, L. Sues 1 Attn: RAWF, Haywood Webb 1 Attn: RAWED</p>	<p>Operations Analysis, SAC Offutt AFB, Nebr. 1 Attn: Mr. E. A. Jackson</p> <p>Commander, AFSC L. G. Hanscom Field Bedford, Mass. 1 Attn: Dr. L. M. Hollingsworth Electronic Res. Directorate</p> <p>AF Command and Control Dev't Div. L.G. Hanscom Field Bedford, Mass. 1 Attn: CCSIL</p> <p>Commander AFRL-ARDC L.G. Hanscom Field Bedford, Mass. 1 Attn: CRNCPV</p> <p>Hq. USAF (AFPRD-NJ-3) Rm 4D-735, The Pentagon Washington 25, D.C. 1 Attn: Mr. Harry Mulky</p> <p>Hq. AFSC Andrews AFB Washington 25, D.C. 1 Attn: SCSEI</p> <p>Department of Defense Defense Communications Agency Washington 25, D.C. 1 Attn: 121A, Tech. Library</p> <p>Director Weapons Systems Evaluation Group Rm 1E875, The Pentagon 1 Washington 25, D.C.</p> <p>Central Intelligence Agency ***2 Washington 25, D.C.</p> <p>Advisory Group on Electron Devices 346 Broadway New York 13, N.Y. 2 Attn: Harry Sullivan</p> <p>Advisory Group on Reliability of Electronic Equipment Office of Asst. Secy. of Def. The Pentagon 1 Washington 25, D.C.</p> <p>DDC (TISIA) Cameron Station 10 Alexandria, Va.</p> <p>U.S. Army Materiel Command Harry Diamond Labs Connecticut Ave. and Van Ness St., N.W. Washington 25, D.C. 1 Attn: Library</p> <p>Director U.S. Nat'l Bureau of Standards Washington 25, D.C. 1 Attn: G. Shapiro, Sec. 14.1</p> <p>Director National Security Agency Ft. George G. Meade, Md. 2 Attn: C 3/TDL 1 Attn: R 304, W. R. Boenning 1 Attn: C 15 1 Attn: R 42</p>
--	--	--

Systems Techniques 2-64

Chief  
U. S. Army Security Agency  
Arlington 12, Va.  
1 Attn: IACON

University of California  
Dept. of Electrical Engineering  
Los Angeles, Calif.  
\*1 Attn: C. T. Leondes  
\*1 Attn: R. S. Elliott

University of California  
Laurence Radiation Lab  
P.O. Box 808  
Livermore, Calif.  
1 Attn: Clovis G. Craig, TJD

Columbia Radiation Lab  
Columbia University  
538 W. 120th St.  
New York 27, N.Y.  
\*1 Attn: D. L. Haricov

University of Chicago  
Labs for Applied Sciences  
Museum of Science and Industry  
Chicago 37, Ill.  
1 Attn: Librarian  
1 Attn: Central Doc. Control-199

Illinois Institute of Tech.  
3501 S. Dearborn St.  
Chicago 16, Ill.  
1 Attn: Security Officer  
Electronics Res. Lab.

Carlyle Barton Labs  
Johns Hopkins University  
Charles and 34th Streets  
Baltimore 18, Md.  
1 Attn: Librarian

MIT Electronic Systems Lab  
Cambridge 39, Mass.  
1 Attn: J. E. Ward

University of Michigan  
Cooley Electronics Lab  
Electrical Engineering Dept.  
Ann Arbor, Mich.  
1 Attn: Dr. D. F. Barton

Director  
Research Division  
New York University  
New York, N.Y.  
1 Attn: R. F. Cotel'essa

The Ohio State University  
Res. Foundation  
1314 Ketter Rd.  
Columbus, Ohio 43212  
1 Attn: R. A. Fouty

Stanford Research Institute  
Menlo Park, Calif.  
\*1 Attn: External Reports, G-037

ERL, SUFC  
P.O. Box 26, University Station  
Syracuse, N.Y.  
1 Attn: T. F. Curry

Defense Systems Lab  
Syracuse University Res. Corp.  
P.O. Box 26, University Station  
Syracuse, N.Y.  
1 Attn: Mr. B. E. Simmons

Defense Research Lab  
P.O. Box 8029  
University of Texas  
1 Austin, Texas

Military Physics Res. Lab.  
University of Texas  
P.O. Box 8936, University  
Station  
Austin 12, Texas  
1 Attn: Mrs. O. G. Williams

Aldermen Library  
University of Virginia  
\*Charlottesville, Va.  
1 Attn: J. C. Myllie

Aerospace Corp.  
P.O. Box 25055  
Los Angeles 45, Calif.  
1 Attn: Dr. Roy Ward

Alpharome Instruments Lab  
Walt Whitman Rd.  
Melville, N.Y.  
1 Attn: Librarian

American Electronics Labs., Inc.  
P.O. Box 552  
Laradale, Pa.  
1 Attn: Librarian

Cornell Aeronautical Labs  
4455 Genesee St.  
Buffalo 21, N.Y.  
1 Attn: D. K. Plummer  
1 Attn: J. P. Desmond, Librarian

Fairchild Semiconductor  
Res. and Dev. Labs  
4001 Junipero Serra Blvd.  
\*Palo Alto, Calif.  
1 Attn: Dr. Grinich

General Electric Co.  
Research Labs  
P.O. Box 1088  
Schenectady, N.Y.  
1 Attn: R. U. Shuey, Mgr.

The Hallicrafters Co.  
4401 W. 5th Ave.  
Chicago 24, Ill.  
1 Attn: Security Librarian

HRB-Singer, Inc.  
1 State College, Pa.  
1 Attn: Conrad L. Welch  
2 Attn: Richard Mollo

Hughes Aircraft Co.  
Documents Center  
Bldg. 6, Rm C2048  
Florence at Teale St.  
Culver City, Calif.  
1 Attn: Tech. Library

ITT Corporation  
ITT Labs Div.  
492 River Rd.  
Nutley, N.J.  
1 Attn: J. LeGrand

ITT Corp.  
ITT Fed. Labs Div.  
500 Washington Ave.  
Nutley, N.J.

Tech. Reports Center  
IBM Corp.  
Space Guidance Center  
Federal Systems Div.  
Owego, N.Y.

Janaky and Pally, Inc.  
1359 Wisconsin Ave., N.W.  
Washington 7, D.C.  
1 Attn: Mr. J. Renner

Lockheed Aircraft Corp.  
Scientific Tech. Info.  
Dept. 72-34  
1 Marietta, Ga.

Loral Electronics Corp.  
825 Bronx River Ave.  
New York 72, N.Y.  
1 Attn: Louise Daniels,  
Librarian

Melpar, Inc.  
3000 Arlington Blvd.  
Falls Church, Va.  
1 Attn: Librarian

Motorola, Inc.  
1430 N. Cicero Ave.  
Chicago 51, Ill.

Motorola, Inc.  
Semiconductor Products Div.  
5005 E. McDowell Rd.  
Phoenix, Ariz.  
1 Attn: Military Marketing Dept.

North American Aviation, Inc.  
Engineering Tech. Library  
Los Angeles 64, Calif.  
1 Attn: D. R. Bracha

Packard Bell Electronics  
P.O. Box 337  
1 Newbury Park, Calif.

Packard Bell Electronics  
12333 W. Olympic Blvd.  
Los Angeles 45, Calif.  
1 Attn: Security Officer

Radio Corp. of America  
75 Varick St.  
New York 13, N.Y.  
1 Attn: G. Muligano

Radio Corp. of America  
DEP and DSD Eng. Library, 304/3  
8500 Balboa Ave.  
Van Nuys, Calif.  
1 Attn: L. R. Mund, Librarian

The RAND Corp.  
1700 Main St.  
Santa Monica, Calif.  
1 Attn: Librarian

Raytheon Co.  
406 E. Gutierrez Ave.  
P.O. Box 636  
1 Santa Barbara, Calif.

Revere Copper and Brass, Inc.  
Foil Div.  
196 Diamond St.  
Brooklyn 22, N.Y.  
1 Attn: Vincen. B. Lane

Sanders Assoc., Inc.  
95 Canal St.  
Nashua, New Hampshire  
1 Attn: Mr. G. Steeg

Scope, Inc.  
121 Fairfax Dr.  
1 Falls Church, Va.

Smyth Res. Associates  
3535 Aero Court  
San Diego 11, Calif.  
1 Attn: Security Officer

Sperry Gyroscope Co.  
Division of Sperry Rand Corp.  
Great Neck, N.Y.  
1 Attn: Mail Sta F-7  
(Mr. K. H. Barney)

Sperry Microwave Electronics Co.  
P.O. Box 1828  
Clearwater, Fla.  
1 Attn: Dr. J. E. Pippin

Lockheed Electronics Co.  
Military Systems  
U.S. Highway No. 22  
Plainfield, N.J.  
1 Attn: C. L. Optiz

Commanding Officer  
U.S. Army Signal Electronic Res. Unit  
P.O. Box 205  
St. View, Calif.

Sylvania Electronic Systems  
Waltham Labs  
100 First Ave.  
Waltham 54, Mass.  
1 Attn: Librarian

Systems Development Corp.  
2500 Colorado Ave.  
Santa Monica, Calif.  
1 Attn: Library, R. Lunney

Ohio University  
College of Applied Sciences  
\*Athens, Ohio  
1 Attn: H. L. Hoffee

Hughes Aircraft Co.  
\*Culver City, Calif.  
1 Attn: Dr. N. I. Hall  
Vice President, Engineer

Space Systems Division  
Air Force Systems Command  
Air Force Unit Post Office  
Los Angeles 45, Calif.  
1 Attn: SSD/SSTRG  
Cap't. Robert D. Eaglett

\* Unclassified Reports Only  
\*\* Quarterly Status Reports Only  
\*\*\* Via - Opal Cook



SPECIAL  
DISTRIBUTION LIST  
for  
Technical Report No. 2303-1  
by  
J. W. Goodman

No. of  
Copies

20	Defense Documentation Center Cameron Station Alexandria, Va.
6	Hq., Space Systems Division Air Force Unit P.O. Los Angeles 45, Calif. 90045
1	SSTRT-Capt. Eaglet
1	SSTK
2	Aerospace Corporation P.O. Box 95185 Los Angeles 45, Calif. 90045
1	Attn: Dr. Roy Ward
1	Attn: Dr. Jack Munushian
1	Attn: Dr. Earle Mayfield
1	Attn: Mr. Edward Soltwedel
1	Attn: Dr. Harry Wessly
1	Attn: Dr. Maier Margolis
1	Attn: Dr. John LeLangre
1	Air Force Avionics Lab Wright-Patterson AFB, Ohio
1	Attn: AVP- Mr. Ray McCormick
1	Attn: AVNT- Mr. Jerry Pasek
2	Secretariat of Special Group on Optical Masers Advisory Group on Electron Devices 346 Broadway New York 13, N.Y.
1	University of Utah Physics Department (Prof. Haycock) c-o Security Officer 310 Park Bldg. Salt Lake City, Utah
1	University of Southern Calif. EE Dept. University Park Los Angeles 7, Calif. 90007 Attn: Dr. Z. Kaprielian